

Zr-MOF-N=CH-C₆H₄-OSO₃H catalyst for the construction of new substituted 4-aminocoumarin analogs

Masoumeh Goudarzvand Chegini , Masoud Mokhtary* , Afshin Pourahmad 

Department of Chemistry, Rasht Branch, Islamic Azad University, Rasht, Iran.

*Corresponding author: mmokhtary@iaurasht.ac.ir

Original Research

Abstract:

Received:
16 December 2023
Revised:
30 January 2024
Accepted:
02 April 2024
Published online:
11 May 2024

In this study, the preparation of a new functionalized acidic metal-organic framework nanocatalyst formulated as Zr-MOF-N=CH-C₆H₄-SO₃H has been reported. After characterization using different analysis methods such as FT-IR, XRD, SEM, EDX, TGA, and TEM, the average size of the nanoparticles was found to be between 42.5 and 50.4 nm in diameter. The Nanocatalyst was utilized in the synthesis of novel substituted 4-aminocoumarin analogs via one-pot three-component reaction of 4-aminocoumarin, arylaldehyde or 3-(2-aryldiazenyl)-2-hydroxybenzaldehyde, and 6-hydroxyuracil or 1,3-dimethylbarbituric acid in good-to-excellent yields in ethanol at reflux conditions. A λ_{max} of 362.7 nm was observed for compound **4e**. Simple work-up of the process, mild reaction conditions, no by-products and easy reusability of the nanocatalyst are some of the advantages of the procedure.

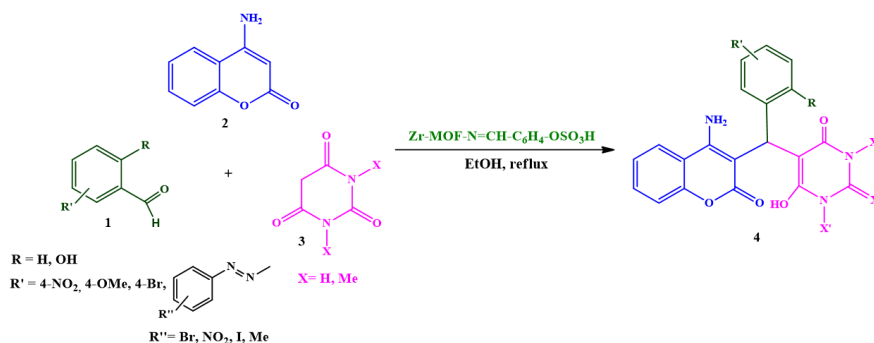
© The Author(s) 2024

Keywords: One-pot reaction; 4-Aminocoumarin; Azo dyes; Metal-organic framework; Nanocatalyst

1. Introduction

Coumarin-based heterocycles have fascinated more investigation due to their antibacterial and antioxidant activities [1], dipeptidyl peptidase-IV (DPP-IV) inhibitors [2], α -glucosidase inhibitor [3], anti-cancer agent [4, 5], anti-Alzheimer [6], cytotoxic, anti-oxidant [7], anti-coagulants [8], anti-tumor [9], anti-hyperglycemic and anti-adipogenic [10]. So, different methods have been reported for their synthesis using various catalysts such as ZnCl₂/POCl₃ [11], piperidine/microwave irradiation [12], PhI(OAc)₂ [13], Pd(OAc)₂ [14], CuOAc [15], Cr(NO₃)₃·9H₂O [16], and [Msim]HSO₄ [17]. Metal-organic frameworks (MOFs), with a variety of topologies and pore sizes, are composed of metal ions/clusters (inorganic nodes) and organic linkers and have received the most from scientists. The metallic clusters are formed by monovalent (Ag⁺, Cu⁺, Na⁺, K⁺, ...), divalent (Zn²⁺, Ni²⁺, Fe²⁺, Mg²⁺, Mn²⁺, Co²⁺, Cu²⁺, Cd²⁺, ...), trivalent (Cr³⁺, Fe³⁺, Al³⁺, Sc³⁺, In³⁺, ...), or tetravalent (Ti⁴⁺, Zr⁴⁺, Hf⁴⁺) metals [18, 19]. Metal-organic frameworks have potential as heterogeneous catalysts because of their tunable porosity, high surface area,

and diversity in metal and functional groups, making them particularly attractive for use as catalysts [20–23]. Azo dyes are applied in the pharmaceutical, cosmetic, food, textile, and leather industries [24–26]. Coumarin-based azo dyes have different properties, such as corrosion inhibitors for mild steel [27], antimicrobial activity [28], and sensitive detection of AcO[−] and CN[−] anions in a semi-aqueous environment [29]. 4-Aminocoumarin is used for the preparation of a variety of five-, six-, and eight-membered fused heterocycles which exhibit various biological and pharmaceutical properties [30–32]. We previously reported the deployment of new procedures for the construction of azo compounds [33, 34]; here, we will investigate Zr-MOF-N=CH-C₆H₄-OSO₃H as a new functionalized acidic MOF nanocatalyst in the synthesis of a series of 4-aminocoumarin analogs via one-pot reaction of 3-(2-aryldiazenyl)-2-hydroxybenzaldehyde or arylaldehyde, 4-aminocoumarin, and 6-hydroxyuracil/1,3-dimethyl barbituric acid in ethanol under reflux conditions (Scheme 1).



Scheme 1. Construction of substituted 4-aminocoumarin analogs.

2. Experimental

2.1 Material and methods

All the chemical compounds were obtained from Merck. NMR and FT-IR spectra were carried out by a Bruker Avance DRX 300 MHz in $(\text{CD}_3)_2\text{SO}$ solvent and an IR-470 spectrometer, respectively. UV-Vis's data of the compounds were recorded with a Rayleigh-UV2601 spectrophotometer. FE-SEM observations were recorded on MIRA3 at 15 kV. TEM analysis was performed on a Philips CM10 equipment at 100 kV. The EDS analysis of the nanocatalyst was accomplished by a TESCAN (MIRA II) microscope at a voltage of 20 kV. The crystalline structure of the nanocatalyst was determined by Philips (PW1730), XRD instrument at $\lambda=1.54056 \text{ \AA}$. Thermogravimetric investigation (TGA, Q600) was recorded in an inert atmosphere at 25-800 °C and a 10 °C/min heating rate.

2.2 Preparation of Zr-MOF-N=CH-C₆H₄-OSO₃H nanocatalyst

Zr-MOF-NH₂ was produced as stated by the previously introduced procedure [35]. Then, 1g of Zr-MOF-NH₂ was suspended in 20 mL of ethanol, and 4-hydroxybenzaldehyde (10 mmol, 1.22 g) was added to the mixture and refluxed for 3 h. After filtration, a yellow solid (Zr-MOF-N=CH-C₆H₄-OH) was obtained, which was then washed with ethanol and dried for further usage. Then, 1 g of the obtained solid was suspended in 30 mL of CHCl₃, and then chlorosulfuric acid (5 mmol, 0.33 mL) was added gradually to the mixture and stirred for 2 h at 25 °C. The solid was dried under a vacuum at 25 °C.

2.3 Synthesis of 4-aminocoumarin

4-aminocoumarin was prepared by reaction of 4-hydroxycoumarin (1 mmol) and ammonium acetate (2 mmol) in solvent-free conditions at 130 °C for 3 h. After that, the reaction mixture was cooled to 25 °C, and 10 mL distilled water was added to the mixture, and the obtained solid was filtrated. Then, the obtained precipitate was recrystallized in ethanol solvent.

2.4 General method for the production of 4-aminocoumarin analogs

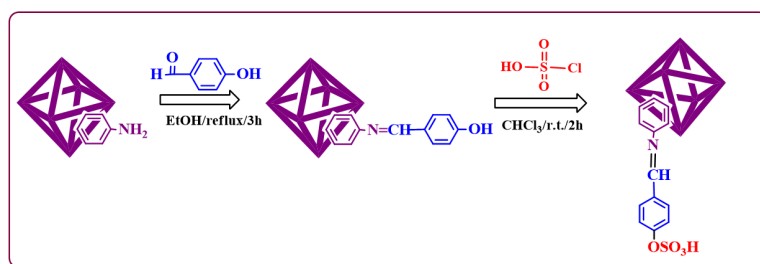
To an equimolar solution of 4-aminocoumarin (1 mmol), 2-hydroxy-5-(aryldiazenyl) benzaldehyde (1 mmol), and 6-hydroxyuracil or 1,3-dimethylbarbituric acid (1 mmol) in 5 mL of ethanol, 0.04 g of Zr-MOF-N=CH-C₆H₄-OSO₃H was added under reflux conditions. The reaction progress was periodically observed by TLC (EtOAc/*n*-hexane/MeOH, 3:8:1). After the end of the condensation, the nanocatalyst was filtrated and washed with hot EtOH (2×10 mL). The pure compound was prepared by recrystallization with ethanol.

3. Results and discussion

3.1 Characterization of Zr-MOF-N=CH-C₆H₄-OSO₃H

In this research, acidic metal-organic framework (Zr-MOF-N=CH-C₆H₄-OSO₃H) catalyst was prepared by the reaction of Zr-MOF-N=CH-C₆H₄-OH with chlorosulfuric acid in CHCl₃ at room temperature (Scheme 2).

The FT-IR spectra of the Zr-MOF-NH₂, Zr-MOF-N=CH-C₆H₄-OH, and Zr-MOF-N=CH-C₆H₄-OSO₃H are shown in Figure 1. The asymmetric and symmetric stretching of SO₂ can be concluded with the bands perceived in 1272



Scheme 2. Synthetic routes for the production of Zr-MOF-N=CH-C₆H₄-OSO₃H.

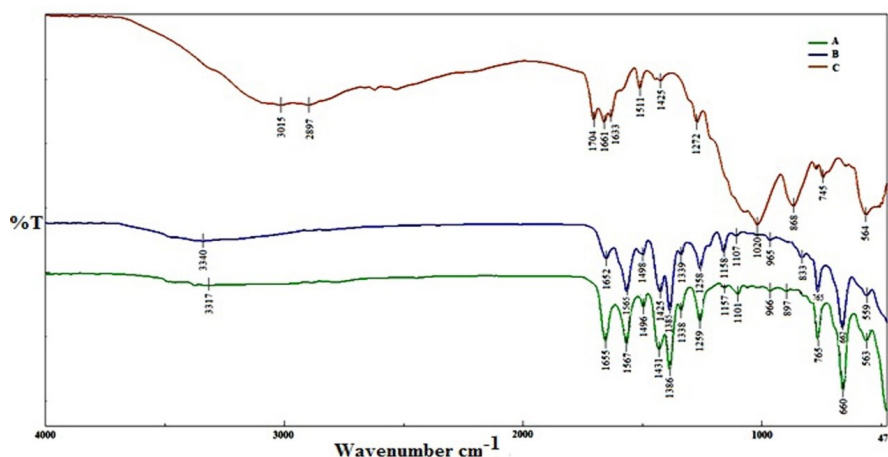


Figure 1. FT-IR spectra of: (A) Zr-MOF-NH₂, (B) Zr-MOF-N=CH-C₆H₄-OH, and (C) Zr-MOF-N=CH-C₆H₄-SO₃H.

and 1020 cm⁻¹, respectively. The wave numbers of 1633, 1661, and 1704 cm⁻¹ were related to the stretching vibration of C=C, C=N, and C=O, respectively, and the wide peak at 3015-2897 cm⁻¹ was assigned to the OH stretching of SO₃H functional group and confirmed the formation of Zr-MOF-N=CH-C₆H₄-OSO₃H (Fig. 1(C)).

3.2 XRD analysis

The XRD spectra of Zr-MOF-NH₂, Zr-MOF-N=CH-C₆H₄-OH, and Zr-MOF-N=CH-C₆H₄-OSO₃H are introduced in Figure 2. The characteristic XRD peaks of Zr-MOF-NH₂ displayed that the observed peaks related to the Zr-MOF-NH₂ pattern [35]. The XRD pattern of Zr-MOF-N=CH-C₆H₄-OSO₃H showed the diffraction peaks correspond to the harmonic pattern of Zr-MOF. Three peaks located at 2θ of 7.4°, 7.7°, and 25.7° are associated with the diffraction by (111), (200) and (600) planes [35]. Also, the original crystalline phase structure was maintained in Zr-MOF-N=CH-C₆H₄-OSO₃H after functionalization.

3.3 FE-SEM analysis

The morphologies of the prepared Zr-MOF-N=CH-C₆H₄-OSO₃H that were characterized by using FE-SEM are presented in Figure 3. According to the FE-SEM images of the nanocatalyst, the particles of Zr-MOF-N=CH-C₆H₄-OSO₃H were almost well dispersed. The average size of the nanoparticles was found between 42.5 and 50.4 nm in diameter.

3.4 EDS characterization

The EDS spectrum of Zr-MOF-N=CH-C₆H₄-OSO₃H shows the presence of carbon, nitrogen, oxygen, sulfur, chlorine, and zirconium components in the nanocatalyst (Fig. 4). Furthermore, the outcome of FE-SEM/mapping are illustrated in Fig. 5. As seen in Fig. 5, C (red), N (white), O (green), S (blue), and Zr (purple) atoms are uniformly distributed on the surface of Zr-MOF-N=CH-C₆H₄-OSO₃H.

3.5 TEM Analysis

TEM was utilized to discover the structure information of the nanocatalyst. The TEM image of the Zr-MOF-N=CH-C₆H₄-OSO₃H shows spherical crystalline nanoparticles as

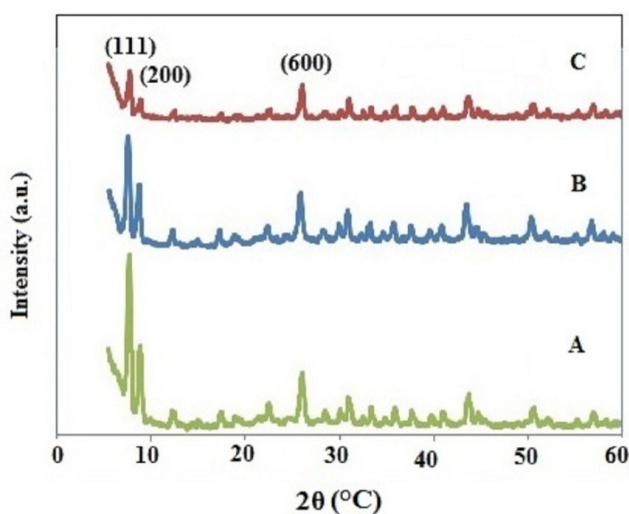


Figure 2. XRD spectra: (A) Zr-MOF-NH₂, (B) Zr-MOF-N=CH-C₆H₄-OH, (C) Zr-MOF-N=CH-C₆H₄-SO₃H.

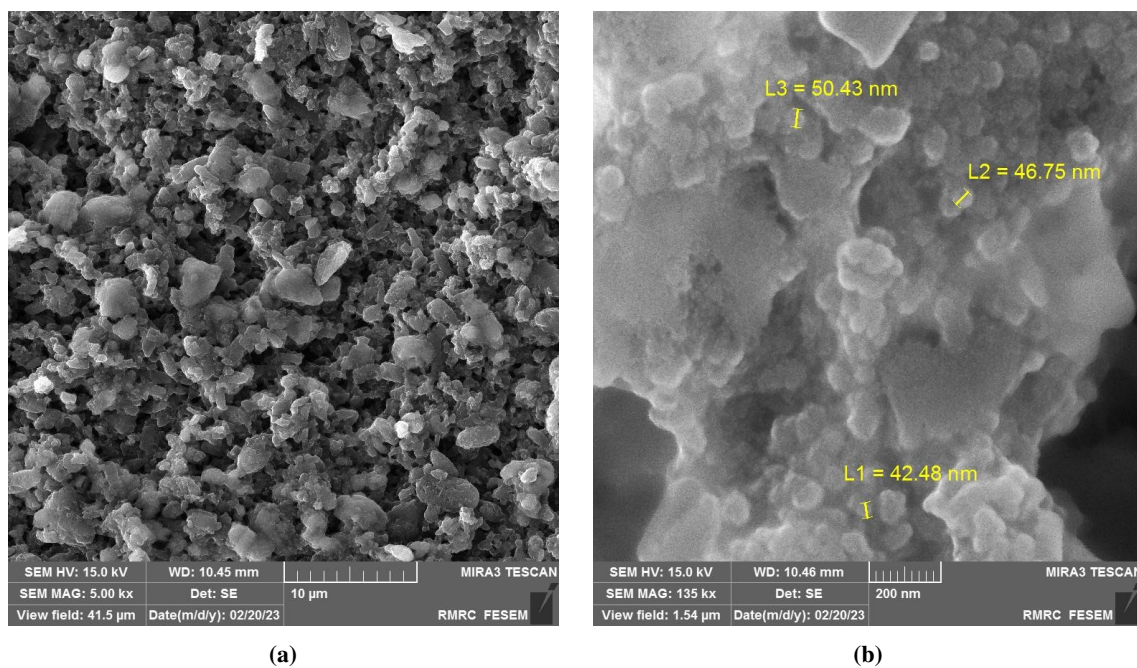


Figure 3. FE-SEM image of Zr-MOF-N=CH-C₆H₄-OSO₃H.

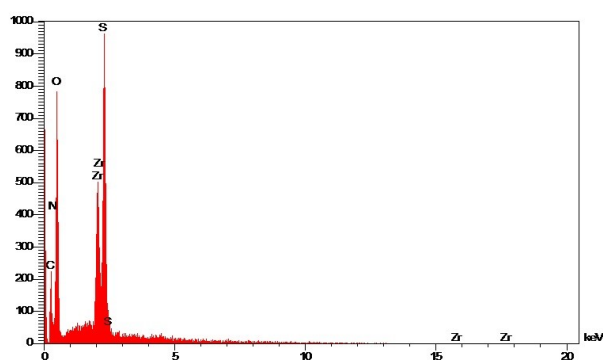


Figure 4. EDS spectrum of Zr-MOF-N=CH-C₆H₄-OSO₃H.

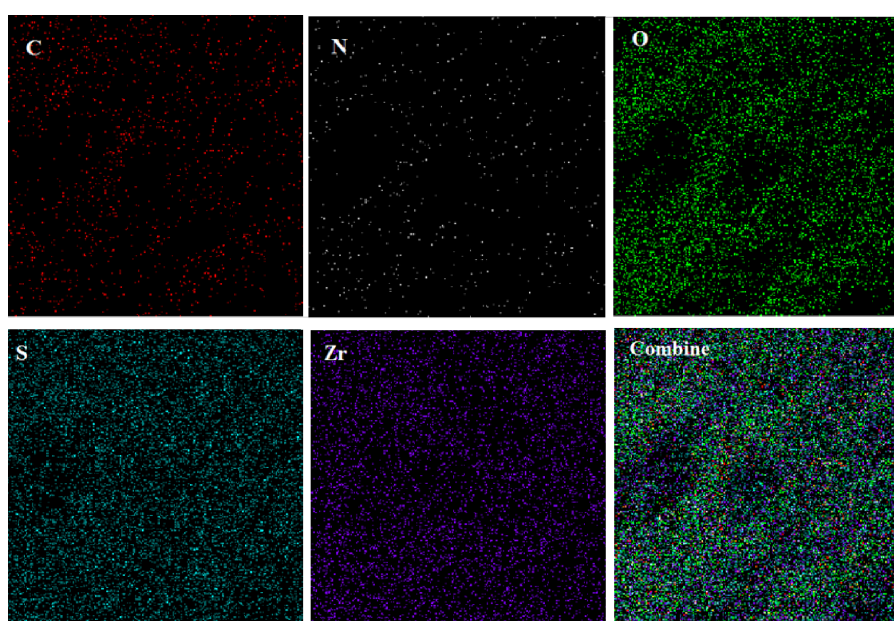


Figure 5. Elemental mapping analysis of Zr-MOF-N=CH-C₆H₄-OSO₃H.

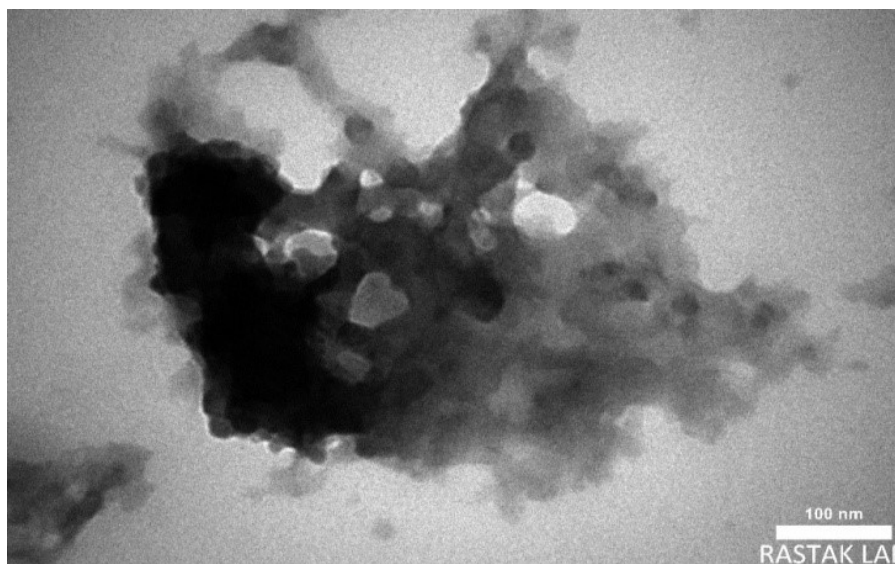


Figure 6. TEM image of the nanocatalyst.

well as grain size of about 40 nm which confirms the nano-sized structure of the prepared catalyst (Fig. 6).

3.6 Thermogravimetric characterization

The TGA-DTG thermogram of the nanocatalyst obtained in the range of 50–800 °C is illustrated in Fig. 7. The mass reduction below 130 °C can be attributed to the elimination of adsorbed solvents or water on the surface. The weight loss at 250 °C corresponds to the breakdown of the band of N=C of the nanocatalyst structure. The weight reduction at 325 °C can be attributed to the dissociation of the band of O-S of the nanocatalyst structure. The significant mass loss that happened at ~533 °C because of the depletion of the Zr-MOF backbone. Thus, the construction of the nanocatalyst is stable up to 250 °C.

3.7 UV-Vis spectra of azo-products

The UV-Vis spectra of azo-products **4d-4l** was obtained in the range of 200 and 800 nm. The UV-Vis absorption of the azo-compounds **4d-4l** illustrated two absorption peaks in 225–400 nm (Fig. 8). A λ_{max} of 362.7 nm was seen for **4e**. The calculated ϵ (molar absorptivity), FWHM (full width at half-maximum), and λ_{max} concluded from the UV-Vis

spectra of azo-products **4d-4l** are illustrated in Table 1. To evaluate the acid strength of Zr-MOF-N=CH-C₆H₄-SO₃H, the nanocatalyst was titrated with NaOH (0.01 mol L⁻¹) in the existence of phenolphthalein. The total acidity of the nanocatalyst was 4.3 mmol g⁻¹. To make the reaction conditions better, the effect of different parameters, including the catalyst amount and solvent effects in the synthesis of **4e** derivatives, were investigated, the results of which are shown in Tables 2 and 3. Experimental results showed that in the lack of the nanocatalyst, the reaction does not generate a product with a good yield. The best results were observed when the reaction was refluxed in ethanol. Using various amounts of catalyst (0.01, 0.02, 0.03, 0.04, and 0.05g) to optimize the reaction process, the effect of the amount of Zr-MOF-N=CH-C₆H₄-OSO₃H

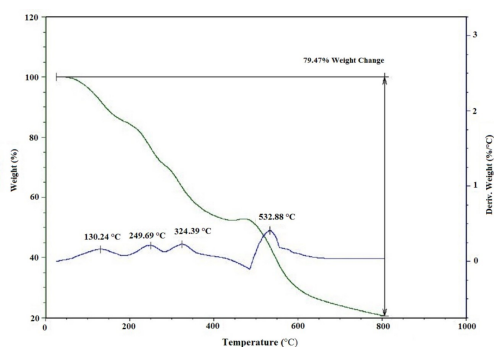


Figure 7. TGA-DTG thermogram of Zr-MOF-N=CH-C₆H₄-SO₃H.

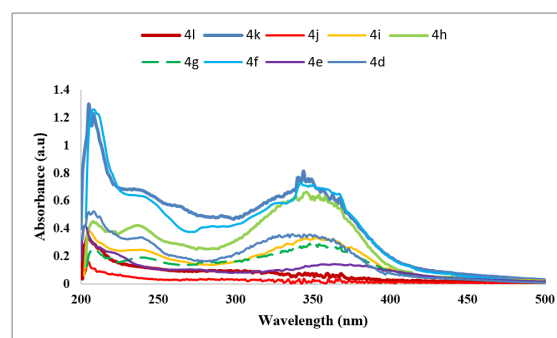


Figure 8. UV-Vis spectra of products **4d-4l**.

Table 1. FWHM, ϵ , and λ_{max} from the UV–Vis data of azoproducts **4d–4l**.

product	ϵ (L.mol ⁻¹ .cm ⁻¹)	FWHM (nm)	ab (a.u)	λ_{max} (nm)
4d	52332	89.33544	0.34888	337.16809
4e	20849	120.66248	0.13899	362.78963
4f	102504	74.38235	0.68336	348.94443
4g	37749	97.54788	0.25166	344.27195
4h	94037	82.66007	0.62691	342.57157
4i	46283	88.86338	0.30855	346.85092
4j	1280	44.75941	0.00853	356.61147
4k	106088	84.63218	0.70725	342.92247
4l	68010	57.7047	0.4534	346.88276

Table 2. Production of **4e** via various solvents^a.

entry	solvent	time (h)	yield (%) ^b
1	ethanol	1.5	95
2	H ₂ O	3	47
3	<i>n</i> -hexane	10	34
4	CHCl ₃	10	42
5	MeCN	10	71

^a Reaction conditions: 2-hydroxy-5-(4-nitrophenyl)diazenylbenzaldehyde (1 mmol), 4-aminocoumarin (1 mmol), 1,3-dimethyl barbituric acid (1 mmol), Zr-MOF-N=CH-C₆H₄-OSO₃H (0.04 g) at reflux conditions.

^b Yield refers to separated products.

Table 3. Production of **4e** in different values of the nanocatalyst^a.

entry	time (h)	nanocatalyst (g)	yield (%) ^b
1	4	0.01	56
2	2.5	0.02	69
3	2	0.03	84
4	1.5	0.04	95
5	1.5	0.05	95

^a Reaction conditions: 2-hydroxy-5-(4-nitrophenyl)diazenylbenzaldehyde (1 mmol), 4-aminocoumarin (1 mmol), 1,3-dimethyl barbituric acid (1 mmol), at reflux conditions in ethanol (5 mL).

^b Yield refers to isolated products.

was explored. The best quantity of the nanocatalyst is 0.04 g, which gave compound **4e** in a 95% yield (Table 3). After obtaining the best conditions for the reaction, various aryl and azo aldehydes, including EWG (electron-withdrawing) and EDG (electron-donating) groups, were subjected to the reactions. All of them produced their corresponding products with high yields (Table 4). This method can be used for gram-scale operations without any problems. The work-up of the reaction mixture is very suitable, which can be easily applied to gram-scale operations. In this regard, we have studied the reaction of 4-aminocoumarin (10 mmol, 1.61 g), 2-hydroxy-5-(4-nitrophenyl) diazenylbenzaldehyde (10 mmol, 2.71 g), and 1,3-dimethylbarbituric acid (10 mmol, 1.56 g) using of Zr-MOF-N=CH-C₆H₄-OSO₃H (0.4 g) in EtOH (75 mL) under reflux conditions.

Through this protocol, the reactions proceeded to completion and the resulting product **4e** was isolated in 95.8% (5.47 g) yields after 100 minutes.

The proposed mechanism for the investigated reaction by Zr-MOF-N=CH-C₆H₄-OSO₃H as an acidic heterogeneous nanocatalyst is shown in Scheme 3. It is presumed that the synthesis may start with the reaction of 2-hydroxy-5-(aryldiazenyl) benzaldehyde with 4-aminocoumarin to produce the intermediate **I**. Actually, the electrophilic strength of the carbonyl group in azo aldehyde increases due to protonation via H⁺ of Zr-MOF-N=CH-C₆H₄-OSO₃H. Then, intermediate **I** is transformed into intermediate **II** through tautomerization. Next, 6-hydroxyuracil or 1,3-dimethylbarbituric acid attacks to intermediate **II** to generate intermediate **III**. Finally, intermediate **III** transforms to

Table 4. Construction of substituted 4-aminocoumarin analogs^a.

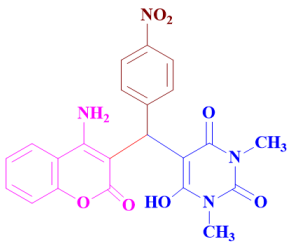
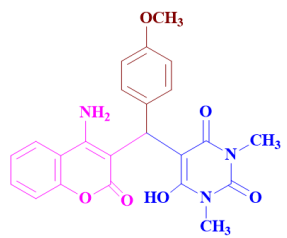
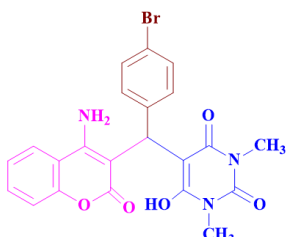
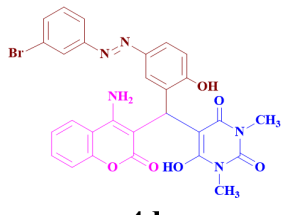
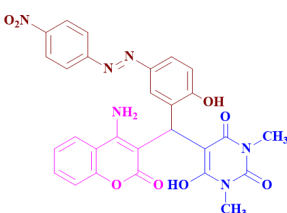
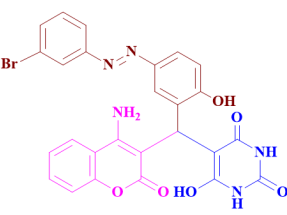
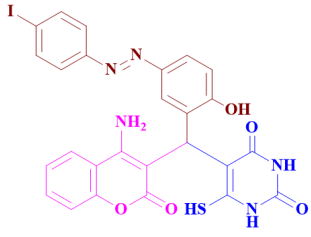
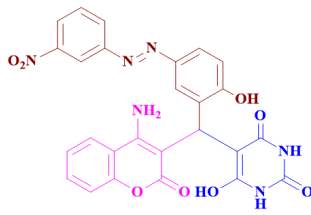
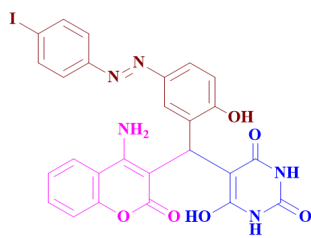
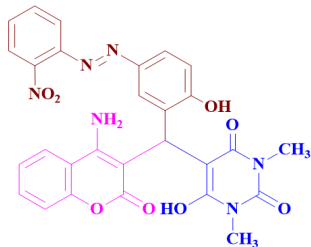
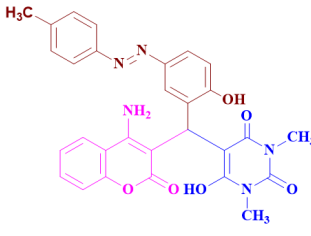
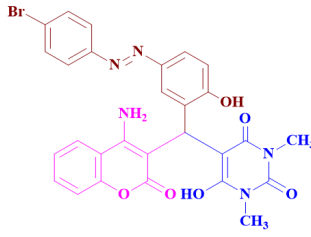
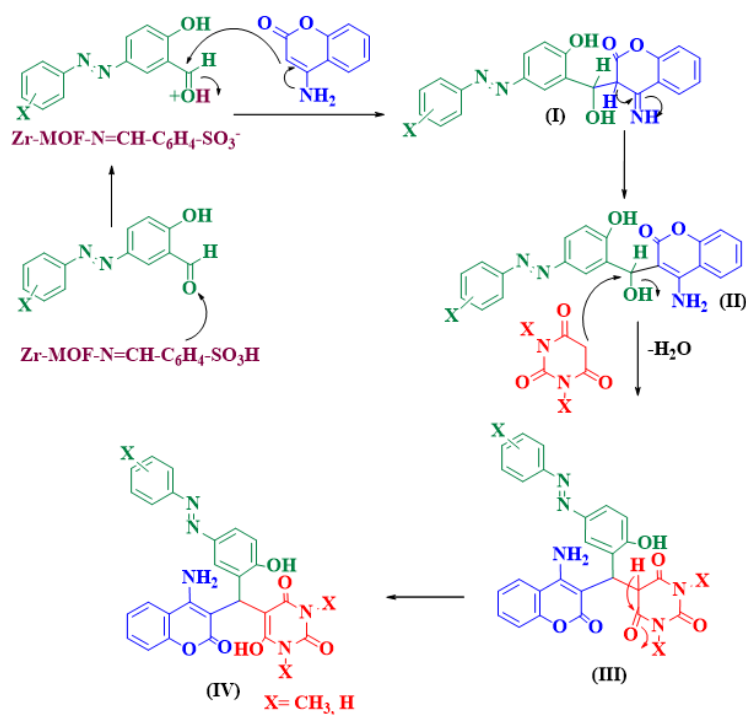
Entry	Product	Time (min)	Yield (%) ^b	Mp (°C)
1	 4a	60	97	206-207
2	 4b	70	94	235-237
3	 4c	60	96	180-182
4	 4d	90	95	> 300
5	 4e	90	96	> 300
6	 4f	95	93	289-291

Table 4. Continued.

Entry	Product	Time (min)	Yield (%) ^b	Mp (°C)
7	 4g	100	92	> 300
8	 4h	90	94	291-293
9	 4i	100	91	> 300
10	 4j	95	92	285-287
11	 4k	110	90	278-280
12	 4l	90	95	> 300

^a Reaction conditions: 2-hydroxy-5-(aryldiazenyl)benzaldehyde or arylaldehyde (1 mmol), 4-aminocoumarin (1 mmol), barbituric acid/1,3-dimethyl barbituric acid (1 mmol), Zr-MOF-N=CH-C₆H₄-OSO₃H (0.04 g) at reflux conditions in ethanol (5 mL).

^b Yield refers to isolated products.



Scheme 3. Possible mechanism for the substituted 4-aminocoumarin analogs.

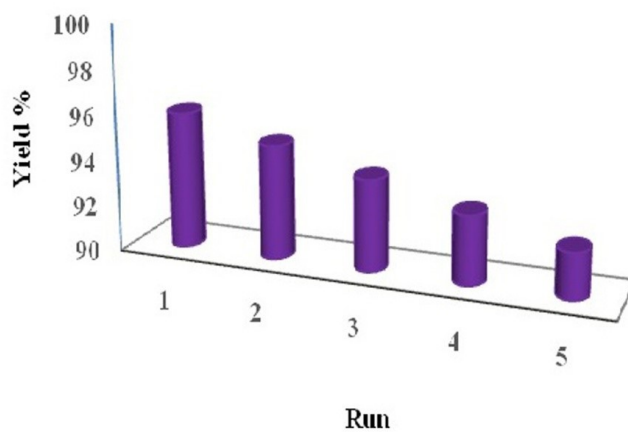


Figure 9. Reusability of Zr-MOF-N=CH-C₆H₄-OSO₃H in the synthesis of product **4e**.

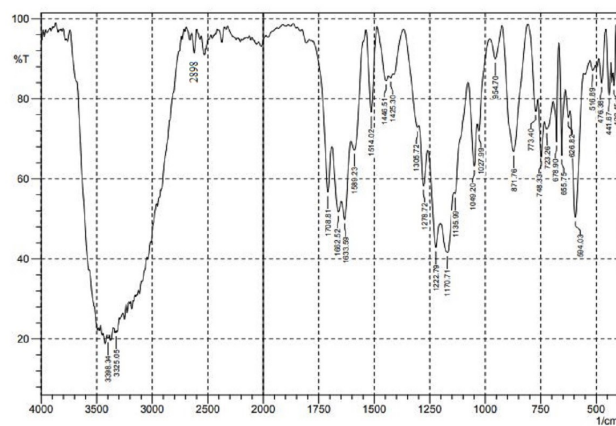


Figure 10. FT-IR spectra of Zr-MOF-N=CH-C₆H₄-SO₃H after 5 runs.

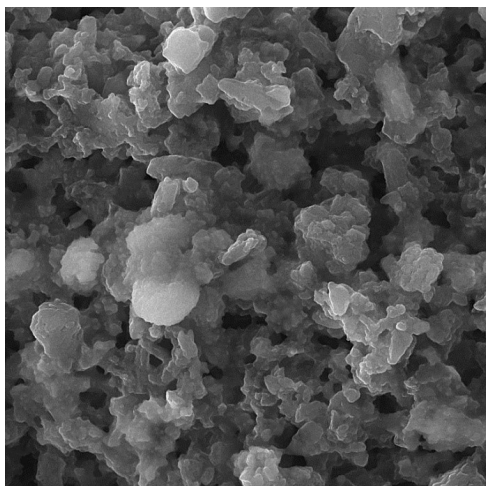


Figure 11. FE-SEM image of Zr-MOF-N=CH-C₆H₄-OSO₃H after 5 runs.

desired product **IV** via tautomerization. Also, Zr-MOF displays an activity as expected for Lewis's acids [36]. The Zr-MOF is containing [Zr₆O₄(OH)₄]¹²⁺ clusters which the Zr has its maximal coordination number of 8. It is noteworthy, the [Zr₆O₄(OH)₄]¹²⁺ cluster depending on the substituents on the 1,4-benzenedicarboxylate linker can be reversibly dehydroxylated to [Zr₆O₆]¹²⁺ at temperatures between 373 and 523 K. This decreases the Zr coordination number from 8 to 7, which still leaves the Zr in a highly coordinated state, with little room for incoming reactants [37].

The reusability of the catalyst was determined in the preparation of **4e**. After completion of the reactions, Zr-MOF-N=CH-C₆H₄-OSO₃H was recycled by filtration, then washed with ethanol and dried at 80 °C for 3 h. This procedure was repeated 5 times for reactions, and no considerable decrease in catalyst property was observed at the same conditions for at least 5 runs (Fig. 9). The stability of the catalyst was explored by FT-IR and SEM analysis. The FT-IR spectrum of the reused catalyst is shown in Fig. 10. As can be seen, there is no change in the FT-IR spectrum of the reused catalyst after 5 times. Furthermore, the obtained results from SEM analysis showed that the morphology of the catalyst did not change after 5 times reuse (Fig. 11).

4. Conclusion

In this project, we have announced a simple procedure for the construction of new substituted 4-aminocoumarin analogs via a one-step reaction using Zr-MOF-N=CH-C₆H₄-OSO₃H as a new functionalized acidic MOF nanocatalyst. Due to the high oxidation state of zirconium (IV) in the catalyst frameworks, there is a strong bond between the Zr and the organic layer linkers, so good thermal and chemical stabilities are observed. The optimized conditions promote the reaction under mild conditions to give the desired product in good-to-excellent yields and reasonable reaction times. The attractive features of this work are easy work-up of the process, mild reaction conditions, no by-products, and reusability of the nanocatalyst. Considering the importance of azo compounds, the presented method can be very suitable for the synthesis of azo dyes with high yields.

Acknowledgement

Financial support of Islamic Azad University, Rasht branch is appreciated.

Authors Contributions

All authors have contributed equally to prepare the paper.

Availability of Data and Materials

The data that support the findings of this study are available from the corresponding author upon reasonable request.

Conflict of Interests

The authors declare that they have no known competing financial interests or personal relationships that could have appeared to influence the work reported in this paper.

Open Access

This article is licensed under a Creative Commons Attribution 4.0 International License, which permits use, sharing, adaptation, distribution and reproduction in any medium or format, as long as you give appropriate credit to the original author(s) and the source, provide a link to the Creative Commons license, and indicate if changes were made. The images or other third party material in this article are included in the article's Creative Commons license, unless indicated otherwise in a credit line to the material. If material is not included in the article's Creative Commons license and your intended use is not permitted by statutory regulation or exceeds the permitted use, you will need to obtain permission directly from the OICCPress publisher. To view a copy of this license, visit <https://creativecommons.org/licenses/by/4.0>.

References

- [1] M. Verma, A. Thakur, S. Kapil, R. Sharma, A. Sharma, and R. Bharti. *Mol. Divers*, **27**(2023):889–900. DOI: <https://doi.org/10.1007/s11030-022-10461-1>.
- [2] P.K. Vawhal, S.B. Jadhav, S. Kaushik, K. Charan Panigrahi, C. Nayak, H. Urmee, S.L. Khan, F.A. Siddiqui, F. Islam, A. Eftekhari, A.R. Alzahrani, M. Fakhami Nur Azlina, M. Rahman Sarker, and I. Abdel Aziz Ibrahim. *Molecules*, **28**(2023):1004–1023. DOI: <https://doi.org/10.3390/molecules28031004>.
- [3] M. Aghaei Khouzani, M. Mogharabi, M.A. Faramarzi, S. Mojtavavi, H. Azizian, M. Mahdavi, and S.M. Hashemi. *J. Mol. Struct*, **1282**(2023):135194. DOI: <https://doi.org/10.1016/j.molstruc.2023.135194>.
- [4] B.B. Shaik, N.K. Katari, P. Seboletswe, R. Gundla, N.D. Kushwaha, V. Kumar, P. Singh, R. Karpoornath, and M.D. Bala. *Anti-Cancer Agents, Med. Chem*, **23**(2023):142–63. DOI: <https://doi.org/10.2174/1871520622666220418143438>.
- [5] M.H. Teiten, F. Gaascht, S. Eifes, M. Dicato, and M. Diederich. *Genes Nutr*, **5**(2010):61–74. DOI: <https://doi.org/10.1007/s12263-009-0152-3>.
- [6] L. Piazzini, A. Cavalli, F. Colizzi, F. Belluti, M. Bartolini, F. Mancini, M. Recanatini, V. Andrisano, and A. Rampa. *Bioorg. Med. Chem. Lett*, **18**(2008):423–426. DOI: <https://doi.org/10.1016/j.bmcl.2007.09.100>.
- [7] B. Yuce, O. Danis, A. Ogan, G. Sener, M. Bulut, and A. Yarat. *Arzneimittelforschung*, **59**(2009):129–134. DOI: <https://doi.org/10.1055/s-0031-1296375>.
- [8] A. Kraimi, N. Belboukhari, K. Sekkoum, and H.Y. Aboul-Enein. *Aditum. J. Clin. Biomed. Res*, **2**(2021):1–13. DOI: <https://doi.org/04.2021/1.1027>.
- [9] K.M. Amin, A.M. Taha, R.F. George, N.M. Mohamed, and F.F. Elsenduny. *Archiv. Der. Pharmazie*, **351**(2017):170–199. DOI: <https://doi.org/10.1002/ardp.201700199>.
- [10] A.A. Husain, A.S. Husain, N.D. Gawhale, S.L. Khan, and D.V. Murlidhar. *J. Pharm. Negat. Results*, **13**(2022):739–744. DOI: <https://doi.org/10.1177/11795514211042023>.
- [11] D.G. Myszka and R.P. Swenson. *J. Biol. Chem*, **266**(1991):4789–4797.
- [12] Y.F. Sun and Y.P. Cui. *Dyes Pigm*, **78**(2008):65–76. DOI: <https://doi.org/10.1016/j.dyepig.2007.10.014>.
- [13] M. Waheed, N. Ahmed, M.A. Alsharif, M.I. Alahmdi, and S. Mukhtar. *Chem. Select*, **4**(2019):1872–1878. DOI: <https://doi.org/10.1002/slct.201803927>.
- [14] K. Sasano, J. Takaya, and N. Iwasawa. *J. Am. Chem. Soc*, **135**(2013):10954–10957. DOI: <https://doi.org/10.1021/ja405503y>.
- [15] Y. Yamamoto and N. Kirai. *Org Lett*, **10**(2008):5513–5516. DOI: <https://doi.org/10.1021/ol802239n>.
- [16] M.H. Krishna and P. Thriveni. *Der Pharma Chem*, **8**(2016):94–98.
- [17] N. Ghaffari Khaligh. *Catal. Sci. Technol*, **2**(2012):1633–1636. DOI: <https://doi.org/10.1039/C2CY20196H>.
- [18] H.C. Zhou, H.C. Zhou, J.R. Long, and O.M. Yaghi. *Chem. Rev*, **112**(2012):673–674. DOI: <https://doi.org/10.1021/cr300014x>.
- [19] A. Albouyeh, A. Pourahmad, and H. Kefayati. *J. Coord. Chem*, **74**(2021):2174–2184. DOI: <https://doi.org/10.1080/00958972.2021.1954173>.
- [20] H. Sephehramansourie, H. Alamgholiloo, M.A. Zolfigol, N. Noroozi Pesyan, and M. Mohammadi. *ACS Sustainable Chem. Eng*, **11**(2023):3182–3193. DOI: <https://doi.org/10.1021/acssuschemeng.2c04810>.
- [21] B. Azari, A. Pourahmad, B. Sadeghi, and M. Mokhtary. *J. Coord. Chem*, **76**(2023):219–231. DOI: <https://doi.org/10.1080/00958972.2023.2166408>.
- [22] M.G. Chegini, M. Mokhtary, and A. Pourahmad. *Polycycl. Aromat. Compd*, (2023):In press. DOI: <https://doi.org/10.1080/10406638.2023.2276238>.
- [23] G. Kumar, A. Dutta, M. Goswami, B. Meena, S. Parasuboyina, R. Nongkhilaw, and D.T. Masram. *J. Mol. Struct*, **1287**(2023):135653. DOI: <https://doi.org/10.1016/j.molstruc.2023.135653>.
- [24] T. Tahir, M. Ashfaq, H. Asghar, M.I. Shahzad, R. Tabassum, and A. Ashfaq. *Mini Rev. Med. Chem*, **19**(2019):708–719. DOI: <https://doi.org/10.2174/1389557518666180727162018>.
- [25] C. Cockerham, A. Caruthers, J. McCloud, L.M. Fortner, S. Youn, and S.P. McBride. *Micromachines*, **13**(2022):577. DOI: <https://doi.org/10.3390/mi13040577>.
- [26] M. Raj and L. Raj. *Orient. J. Chem*, **29**(2013):457464.
- [27] M. Hamizi Yusoff, M. Nurul Azmi, M. Hazwan Hussin, H. Osman, P. Bothi Raja, A. Abdul Rahim, and Kh. Awang. *Int. J. Electrochem. Sci*, **15**(2020):11742–11756. DOI: <https://doi.org/10.20964/2020.12.43>.
- [28] N.N. Ayare, S.H. Ramugade, and N. Sekar. *Dyes Pigm*, **163**(2019):692. DOI: <https://doi.org/10.1016/j.dyepig.2018.12.050>.
- [29] S.K. Dwivedi, S.S. Razia, and A. Misra. *New J. Chem*, **43**(2019):5126–5132. DOI: <https://doi.org/10.1039/C9NJ00004F>.
- [30] R. Miri, R. Motamedi, M. R. Rezaei, O. Firuzi, A. Javidniaand, and A. Shafiee. *Arch. Pharm. Chem. Life Sci*, **344**(2011):111–118. DOI: <https://doi.org/10.1002/ardp.201000196>.

- [31] M. Adib, F. Peytam, M. Rahmanian-Jazi, M. Mohammadi-Khanaposhtani, S. Mahernia, H. R. Bijanzadeh, M. Jahani, S. Imanparast, M.A. Faramarzi, M. Mahdavi, and B. Larijani. *New J. Chem*, **42**(2018):17268–17278. DOI: <https://doi.org/10.1039/C8NJ02495B>.
- [32] M. Foroughi Kaldareh, M. Mokhtary, and M. Nikpassand. *Appl. Organometal Chem*, **34**(2020):e5469. DOI: <https://doi.org/10.1002/aoc.5469>.
- [33] A. Gholami, M. Mokhtary, and M. Nikpassand. *Dyes Pigm*, **180**(2020):108453. DOI: <https://doi.org/10.1016/j.dyepig.2020.108453>.
- [34] M. Dashti, M. Nikpassand, M. Mokhtary, and L. Zare Fekri. *J. Clust. Sci*, **34**(2023):1037–1049. DOI: <https://doi.org/10.1007/s10876-022-02279-6>.
- [35] J. Long, S. Wang, Z. Ding, S. Wang, Y. Zhou, L. Huang, and X. Wang. *Chem. Commun*, **48**(2012):11656–11658. DOI: <https://doi.org/10.1039/C2CC34620F>.
- [36] F. Vermoortele, M. Vandichel, B. Van de Vorde, R. Ameloot, M. Waroquier, V. Van Speybroeck, and D.E. De Vos. *Angew. Chem. Int. Ed*, **51**(2012):4887–4890. DOI: <https://doi.org/10.1002/anie.201108565>.
- [37] J.H. Cavka, S.R. Jakobsen, U. Olsbye, N. Guillou, C. Lamberti, S. Bordiga, and K.P. Lillerud. *J. Am. Chem. Soc*, **130**(2008):13850–13851. DOI: <https://doi.org/10.1021/ja8057953>.